

Supporting Information

Selective naked-eye detection of Hg²⁺ through an efficient turn-on PET fluorescent probe and its real applications

Priyanka Srivastava[†], Syed S. Razi[†], Rashid Ali[†], Ramesh C. Gupta[†], Suresh S. Yadav[‡], G. Narayan[‡] and Arvind Misra^{†*}

[†]Department of Chemistry, Faculty of Science, Banaras Hindu University, Varanasi 221005 Uttar Pradesh, India

*Phone: +91-0542-2307321 ext. 104; +91-0542-6702503. Fax:+91-0542-2368127; +91-0542-2368175 . E-mail: arvindmisra2003@yahoo.com; amisra@bhu.ac.in.

[‡]Department of Molecular and Human Genetics, Faculty of Science, Banaras Hindu University, Varanasi 221005 Uttar Pradesh, India

Table of Contents

1	Materials and Methods	S4-S8
2	Figure S1. ^1H NMR spectrum of 1 in CDCl_3 .	S9
3	Figure S2. ^1H NMR spectrum of 2 in CDCl_3 .	S9
4	Figure S3. ^1H NMR spectrum of 3 in CDCl_3 .	S10
5	Figure S4. ^1H NMR spectrum of 4 in CDCl_3 .	S10
6	Figure S5 (a). ^1H NMR spectrum of 5 in CDCl_3 .	S11
7	Figure S5 (b). ^1H NMR spectrum of 5 in $\text{DMSO}-d^6$.	S11
8	Figure S6. ^{13}C NMR spectrum of 5 in CDCl_3 .	S12
9	Figure S7a. ESI-MS spectrum of 5 in acetonitrile.	S12
10	Figure S7b. HRMS spectrum of 5 .	S13
11	Figure S8. Relative change in (a) absorption and (b) emission spectra of 5 at different pH values 1-14, in HEPES buffer (10 mM; pH 7.0; 70% aqueous ACN). Inset: A pH-emission plot shows change in emission intensity of 5 at pH values, 1 to 14.	S14
12	Figure S9: Change in (b) absorption (c) emission spectra of 5 (10 μM) upon interaction with different metal ions (5.0 equiv) in HEPES buffer (10 mM; pH 7.0; 70% aqueous ACN).	S14
13	Figure S10. Emission spectra of 5 before and after addition of Hg^{2+} (2.5 equiv) in different medium; 70% aqueous-ACN, HEPES (10 mM; pH 7.0), and PBS (10 mM; pH 7.0) buffers.	S15
14	Figure S11. Change in the absorption spectra of a complex 5 - Hg^{2+} , upon interference of tested cations in HEPES buffer (10 mM; pH 7.0; 70% aqueous ACN).	S15
15	Figure S12. (a) Emission spectra of 5 , (b) Interference studies of 5 + Hg^{2+} (2.5 equiv) upon interaction with Fe^{2+} , Fe^{3+} and Mg^{2+} ions (100 equiv) in HEPES buffer (10 mM; pH 7.0; 70% aqueous-ACN) and (c) Bar diagram shows change in emission intensity of 5 upon interaction and interference of tested cation.	S16
16	Figure S13. Change in the emission spectra of 5 by the addition of (a) EDTA to 5 + Hg^{2+} ions (b) Hg^{2+} ions to 5 + EDTA in HEPES buffer (10 mM; pH 7.0; 70% aqueous ACN).	S16
17	Figure S14. Benesi-Hildebrand plot for 5 and Hg^{2+} ions for a 1:2 binding stoichiometry in HEPES buffer (10 mM; pH 7.0; 70% aqueous ACN).	S17
18	Figure S15. (a) Calibration curve for probe 5 and (b) calibration sensitivity plot of 5 toward Hg^{2+} ions in HEPES buffer (10 mM; pH 7.0; 70% aqueous-ACN).	S17
19	Figure S16. FT-IR spectrum of 5 and 5 - Hg^{2+} complex.	S18
20	Figure S17. HRMS spectrum of 5 - Hg^{2+} complex.	S18
21	Figure S18. Emission titration experiment of BSA upon addition of Hg^{2+} ions (λ_{ex} 278 nm) in aqueous NaOAc buffer (50 mM; pH 6.7).	S19
22	Figure S19. (a) Dependence of fluorescence intensity of probe 5 on BSA (0.0- 3.0 μM) and (b) Change in fluorescence spectra of 5 upon addition of BSA (2 μM) and Hg^{2+} (5.0 equiv) in	S19

- HEPES buffer (10 mM; pH 7.0; 70% aqueous ACN).
- 23 **Figure S20.** Emission spectra of **5** with Hg^{2+} acquired before and after addition of Cys in HEPES buffer (10 mM; pH 7.0; 70% aqueous ACN). **S20**
- 24 **Figure S21.** Confocal images of probe **5**+ M^{n+} ($\text{M}^{n+} = \text{Ca}^{2+}, \text{Fe}^{2+}, \text{Mg}^{2+}, \text{Zn}^{2+}$), **5**+ M^{n+} + Hg^{2+} and **5**+ M^{n+} + Hg^{2+} +TPEN (D, E and F; A, B and C are the DIC images of D, E and F respectively). Scale bar represents 100 μm **S20**
- 25 **Figure S22.** Change in emission spectra of **5** upon addition of different anions (50 equiv) in HEPES buffer (10 mM; pH 7.0; 70% aqueous ACN). **S21**
- 26 **Figure S23.** (a) Emission spectra of **5** (a) upon addition of M ions ($\text{Fe}^{2+}, \text{Mg}^{2+}, \text{Ca}^{2+}, \text{Zn}^{2+}$ respectively) followed by PO_4^{3-} and finally Hg^{2+} . Inset : Bar diagram of interaction; (b) upon addition of M ions ($\text{Fe}^{2+}, \text{Mg}^{2+}, \text{Ca}^{2+}, \text{Zn}^{2+}$ respectively) followed by Hg^{2+} and PBS in HEPES buffer (10 mM; pH 7.0; 70% aqueous ACN). **S21**
- 27 **Figure S24.** Emission spectra, bar diagram of relative intensities and truth table of INHIBIT logic gate of probe **5** upon applying inputs of PO_4^{3-} (In_1) and Hg^{2+} (In_2) ions in HEPES buffer (10 mM; pH 7.0; 70% aqueous ACN). **S23**
- 28 **Figure S25.** Emission spectra, bar diagram of relative intensities and truth table of OR logic gate of probe **5** upon applying inputs of Hg^{2+} (In_2) and H^+ (In_3) ions in HEPES buffer (10 mM; pH 7.0; 70% aqueous ACN). **S23**
- 29 **Figure S26.** Emission spectra, bar diagram of relative intensities and truth table of INHIBIT logic gate of probe **5** upon applying inputs of Hg^{2+} (In_2) and EDTA (In_4) in HEPES buffer (10 mM; pH 7.0; 70% aqueous ACN). **S24**
- 30 **Figure S27.** Emission spectra, bar diagram of relative intensities and truth table of INHIBIT logic gate of probe **5** upon applying inputs of H^+ (In_3) and PO_4^{3-} (In_1) in HEPES buffer (10 mM; pH 7.0; 70% aqueous ACN). **S24**
- 31 **Figure S28.** Emission spectra, bar diagram of relative intensities and truth table and symbol of INHIBIT logic gate of probe **5** upon applying inputs of H^+ (In_3) and OH^- (In_5) ions in HEPES buffer (10 mM; pH 7.0; 70% aqueous ACN). **S25**
- 32 **Figure S29.** Emission spectra, bar diagram of relative intensities and truth table of TRANSFER logic gate of probe **5** upon applying inputs of BSA (In_6) and Hg^{2+} (In_2) in HEPES buffer (10 mM; pH 7.0; 70% aqueous ACN). **S25**
- 33 **Table S1-** Truth table of Three TRANSFER, one OR and one INHIBIT logic gate exhibited by probe **5**. **S26**

Materials and Methods: Important chemicals, reagents and solvents were purchased from Merck and Sigma-Aldrich and were used without any further purification. FT-IR spectra in KBr were recorded on a Varian-3100 FT-IR spectrometer. ^1H and ^{13}C NMR spectra (chemical shifts in δ ppm) were recorded on a JEOL AL 300 FT-NMR (300 MHz) spectrometer, using TMS as internal standard. The UV-Vis absorption spectra were recorded on Perkin Elmer 1700 spectrophotometer using a quartz cuvette (path length = 1cm). Fluorescence spectra were recorded on a Cary Eclipse fluorescence spectrophotometer (Varian). Stock solution of probe **5** ($c = 1 \times 10^{-3}$ M) was prepared in HEPES Buffer (10 mM pH 7.0; ACN/H₂O:3:7, v/v). For absorption and emission experiment 150 μL and 30 μL of stock solution was taken and diluted to make the concentrations 50 μM and 10 μM in a 3 mL probe solution. The sensitivity and selectivity of probe **5** toward various class of metal ions (5.0 equiv) such as, Na^+ , K^+ , Ca^{2+} , Zn^{2+} , Pb^{2+} , Ag^+ , Cd^{2+} , Co^{2+} , Ni^{2+} , Fe^{2+} , Fe^{3+} , Cu^{2+} and Hg^{2+} have been examined in HEPES buffer and the optoelectronic behavior of **5** was monitored through the absorption and emission spectroscopy at room temperature. For interaction studies 0.1 M solutions of different metal ions/anions were used.

For ^1H NMR titration experiment solution of probe (1×10^{-2} M) and HgClO_4 was prepared in $\text{DMSO}-d_6$.

Estimation of Quantum Yields. The quantum yield of probe **5** and **5**- Hg^{2+} with respect to standard Quinine sulfate ($\Phi = 0.54$, 1M H_2SO_4) has been estimated in HEPES buffer by the secondary method using equation (1). The absorption and emission spectra of probe **5** and its complex **5**- Hg^{2+} , were studied under similar experimental condition of fluorescence standard (Quinine sulfate) to estimate their respective quantum yields with reference fluorophore.

$$Q = Q_R \cdot I/I_R \cdot OD_R/OD \cdot n^2/n_R^2 \quad (1)$$

Where Q is the quantum yield, I stand for integrated area of fluorescence intensities, OD is optical densities and n is the refractive indexes of solution. The subscript R refers to the reference fluorophore of known quantum yield.

Estimation of Binding Constant and Limit of detection. The Benesi-Hildebrand method was utilized to calculate binding constant for 1:2 stoichiometry between **5** and Hg^{2+} using equation (2).

$$1 / (I - I_o) = 1 / (I - I_f) + 1 / K (I - I_f) [Hg^{2+}]^2 \quad (2)$$

Where K is the association constant, I and I_o are the intensities of **5**, and of a complex, **5**+ Hg^{2+} . I_f is the maximum emission at saturation point.

The limit of detection (LOD) of probe **5** for Hg^{2+} was estimated by equation (3).

$$LOD = 3\sigma(\text{standard deviation for probe } \mathbf{5}) / m (\text{calibration sensitivity}) \quad (3)$$

A linear calibration curve corresponding to change in emission intensities with different concentration of **5** (15.5 to 3.07 μM) has given standard deviation (σ) as 0.041. Similarly, the slope of fluorescence plot corresponding to change in relative fluorescence intensities $\Delta I (I - I_o)$ with different concentration of Hg^{2+} (0 - 8 μM) has given calibration sensitivity (m) 11.91 (Figure S13).

Detection of Hg^{2+} on paper strips and silica coated slide: In order to perform paper strip test small cellulose paper strips ($1.5 \times 0.5 \text{ cm}^2$) (WhatmanTM) were prepared. Each strips were treated with different concentration of probe **5** (5, 1, and 0.2 mM) in HEPES Buffer (10 mM pH 7.0; ACN/ H_2O :3:7, v/v) for 1h and dried in air. Mercury nitrate solution of three different concentrations as, 1×10^{-6} , 1×10^{-7} and 1×10^{-8} M was prepared in water (in each 10 mL of water). Interaction studies were performed by dipping test paper strips of probe **5** in three

different concentration solutions of Hg^{2+} for 5-10 min. Strips were dried in air and then visualized under UV light (at 365 nm).

Similarly, to demonstrate potential application of probe to detect Hg^{2+} on silica coated slides three different concentration of probe **5** has been chosen (1×10^{-4} , 1×10^{-5} , and 1×10^{-6} M) and were adsorbed with the help of fine capillaries on two silica coated slides and dried. On one of the silica coated slides three different concentration of Hg^{2+} (1×10^{-6} , 1×10^{-7} , 1×10^{-8} M) were spread over the spots of probe **5** by spotting method and the air dried slides were visualized under UV light (at, 365 nm).

Synthesis probe 5. Biphenyl methanol (1). Benzophenone was taken in methanol and NaBH_4 (400 mg, 10 mmol) was added slowly to the reaction mixture under ice cold condition. The reaction mixture was stirred for 2h at room temperature and monitored (on TLC). Solvent was evaporated and the precipitate so obtained was washed with water, and dried in air to get compound **1**. Yield 95%. m.p. 69°C . ^1H NMR (CDCl_3) δ (ppm): 7.37-7.23 (m, 10 H), 5.82 (s, 1H), 2.29 (s, -OH). Anal. Calc. for $\text{C}_{13}\text{H}_{12}\text{O}$; C, 84.75%; H, 6.57%. Found: C, 84.62%; H, 6.45%.

Biphenylmethylchloride (2). Compound **1** (300 mg, 1.63 mmol) was taken in DCM and thionyl chloride (213 mg, 1.79 mmol) was added drop wise. The reaction mixture was stirred at room temperature for 5h. After complete reaction (monitored on TLC), excess thionyl chloride was removed by distillation to obtain compound **2** as a yellow color liquid which solidify on cooling. Yield 90%. m.p. $15\text{-}17^\circ\text{C}$. ^1H NMR (CDCl_3) δ (ppm): 7.40-7.22 (m, 10 H), 6.11 (s, 1H). Anal. Calc. for $\text{C}_{13}\text{H}_{11}\text{Cl}$; C, 77.04%; H, 5.47%. Found: C, 77.11%; H, 5.38%.

1-Benzhydrylpiperazine (3). Compound **2** (250 mg, 1.23 mmol) piperazine dihydrochloride (199 mg, 1.25 mmol) and K_2CO_3 (690 mg, 5 mmol) were taken in DMF and the reaction mixture was refluxed overnight. Solvent was removed under reduced pressure. The residue was taken in

water (10 mL) and extracted with ethyl acetate (10 mL x 3 times). The organic layer collected and kept over anhydrous sodium sulfate (30 min) and filtered. Solvent was evaporated under reduced pressure and the crude product so obtained was purified by column chromatography (60–120 mesh; silica gel) using gradient of chloroform : methanol (9:1) as eluent. Yield 80%. m.p. 91-92°C. ¹H NMR (CDCl₃) δ (ppm): 7.38-7.12 (m, 10 H), 4.21 (s, 1H), 2.40 (Br, 4 H). Anal. Calc. for C₁₇H₂₀N₂; C, 80.91%; H, 7.99%; N, 11.10%. Found: C, 80.79%; H, 7.78%; N, 11.27%.

9,10-bischloromethyl anthracene (4). A mixture of anhydrous 1,4-dioxane (35 mL) and conc. HCl (6 mL) was saturated with HCl gas (produced by drop wise addition of conc. HCl to the conc. H₂SO₄). Anthracene (4.45 g, 25 mmol) and paraformaldehyde (3.6 g) were added to the reaction mixture and stirred at 55-60°C. The dispersion of HCl gas and refluxing was continued for 3h at 90°C. The reaction mixture was allowed to stand for 16h to get yellow color solid precipitate. The residue was filtered and washed with dry dioxane (10 mL x 3) to obtain crude product in 68% yield. The product so obtained was recrystallized from toluene to obtain compound **4**. Yield 38%. m.p. 248-250°C. ¹H NMR (CDCl₃) δ (ppm): 8.39 (m, 4H), 7.67 (m, 4H), 5.60 (s, 4H); Anal. Calc. for C₁₆H₁₂Cl₂; C, 69.84; H, 4.40%. Found: C, 69.61; H, 4.53%. ESI-MS; m/z at 276.0 (M+2H)⁺.

9,10-(benzhydrylpiperazine-methyl) anthracene (5). Compound **3** (200 mg, 0.8 mmol), K₂CO₃ (220 mg, 1.6 mmol) and **4** (110 mg, 0.4 mmol) were taken in anhydrous DMF and the reaction mixture was refluxed overnight. After complete reaction (monitored on TLC) solvent was removed under reduced pressure. The residue was taken in water (10 mL) and extracted with ethyl acetate (10 mL x 3 times). The organic layer was washed with water and dried over anhydrous sodium sulfate. The crude product was purified by column chromatography using gradient of ethylacetate / hexane (15 % ; v/v) to obtain compound **5** as light yellow color powder.

Yield 85 %. m.p. 192°C. ¹H NMR (DMSO-*d*₆) δ (ppm): 8.57-8.40 (m, 4H), 7.51-7.48 (m, 4H), 7.36-7.16 (m, 20H, benzene rings), 4.41 (s, 4H, H1'), 4.23 (s, 2H, H3''), 2.55 (s, 4H, H1''), 2.27 (s, 4H, H2''); ¹³C NMR: (75 MHz, CDCl₃) δ (ppm): 142.7, 130.9, 128.3, 127.9, 126.7, 125.5, 124.9, 54.1, 53.5, 52.0; FT-IR: 3026, 2961, 2801, 2757, 1598, 1492, 1447, 1331, 1261, 1136, 1095, 1004, 848, 803, 743, 704, 665. Anal. Calcd. For C₅₀H₅₀N₄: C, 84.95; H, 7.13; N, 7.93%. Found: C, 84.80; H, 7.26; N, 7.71%. ESI-MS; m/z at 708.4 (M+2H)⁺. HRMS (ESI-TOF) m/z: [M+H]⁺ calcd 707.4069 and found 707.4067.

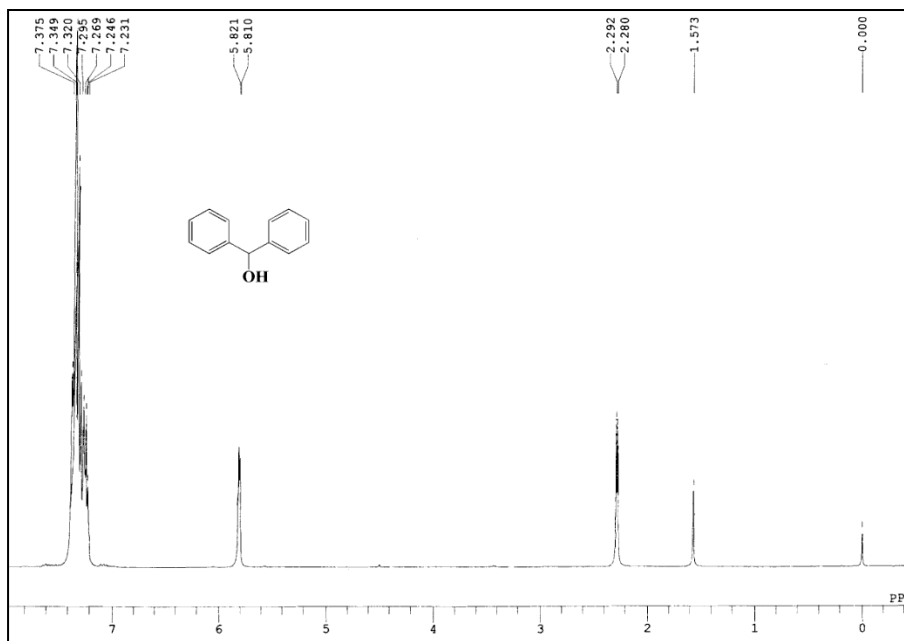


Figure S1. ^1H NMR spectrum of **1** in CDCl_3 .

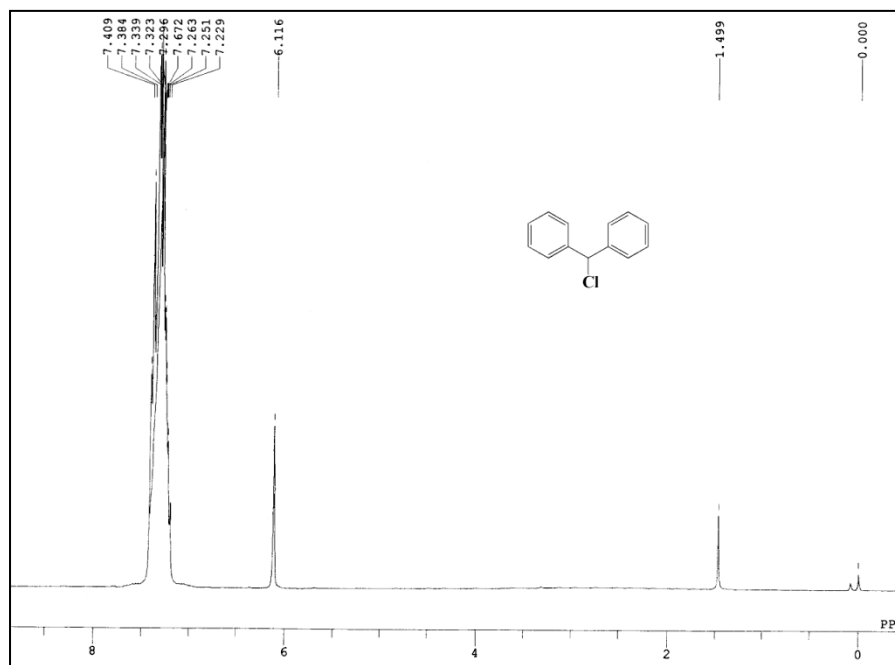


Figure S2. ^1H NMR spectrum of **2** in CDCl_3 .

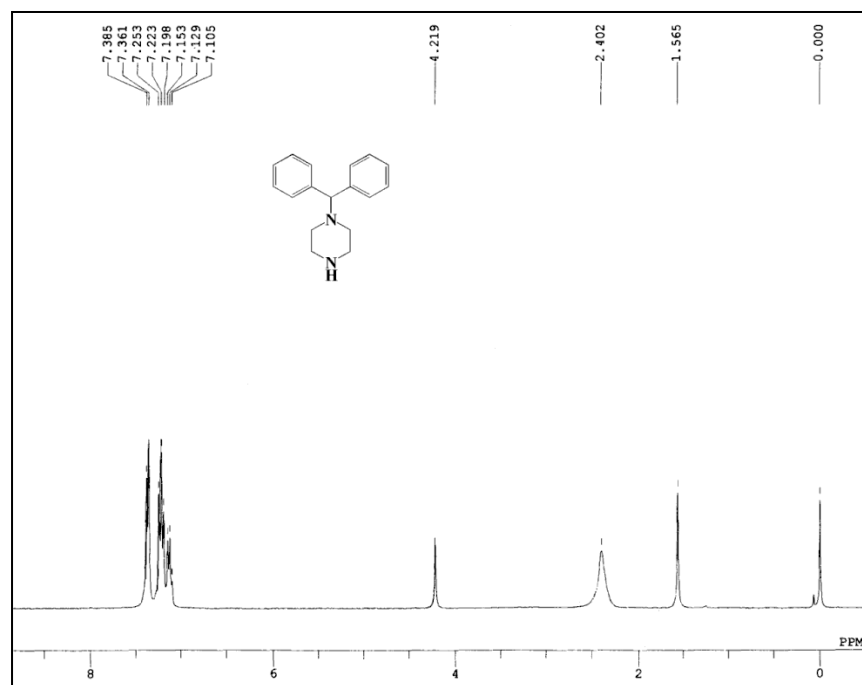


Figure S3. ¹H NMR spectrum of **3** in CDCl₃.

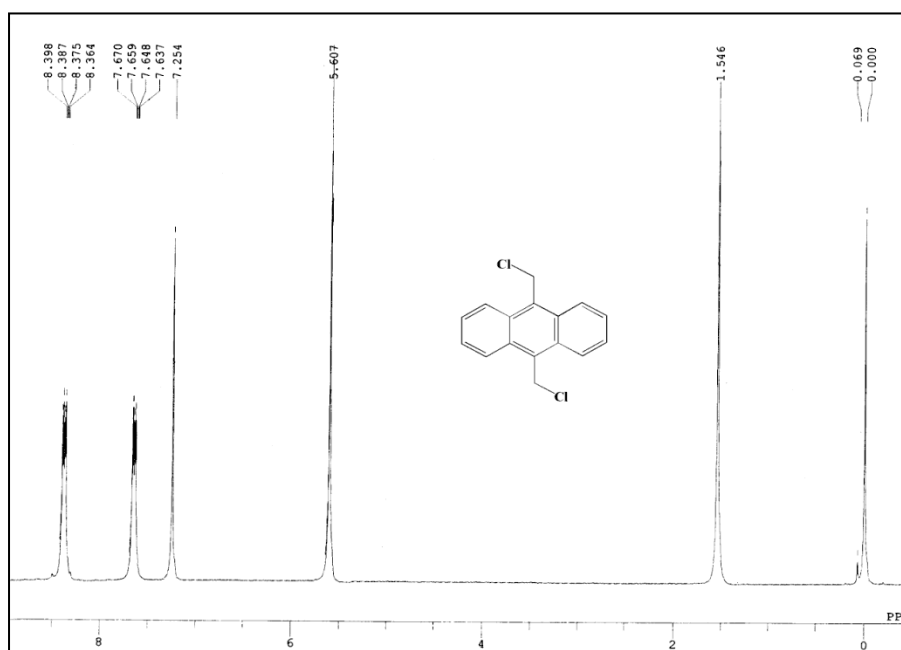


Figure S4. ¹H NMR spectrum of **4** in CDCl₃.

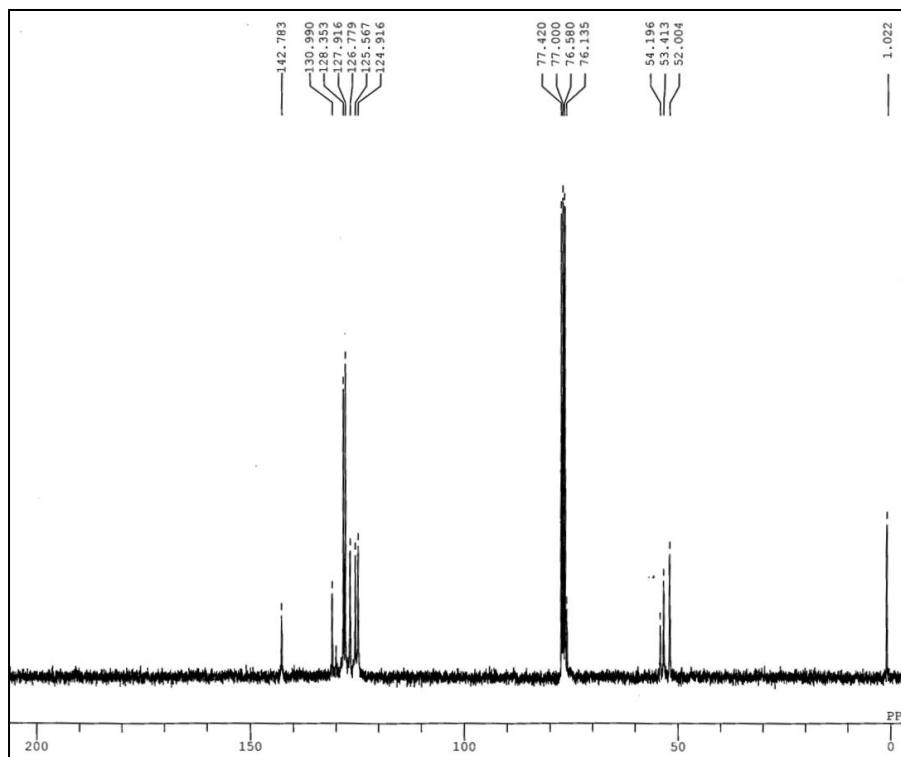


Figure S6. ¹³C NMR spectrum of **5** in CDCl₃.

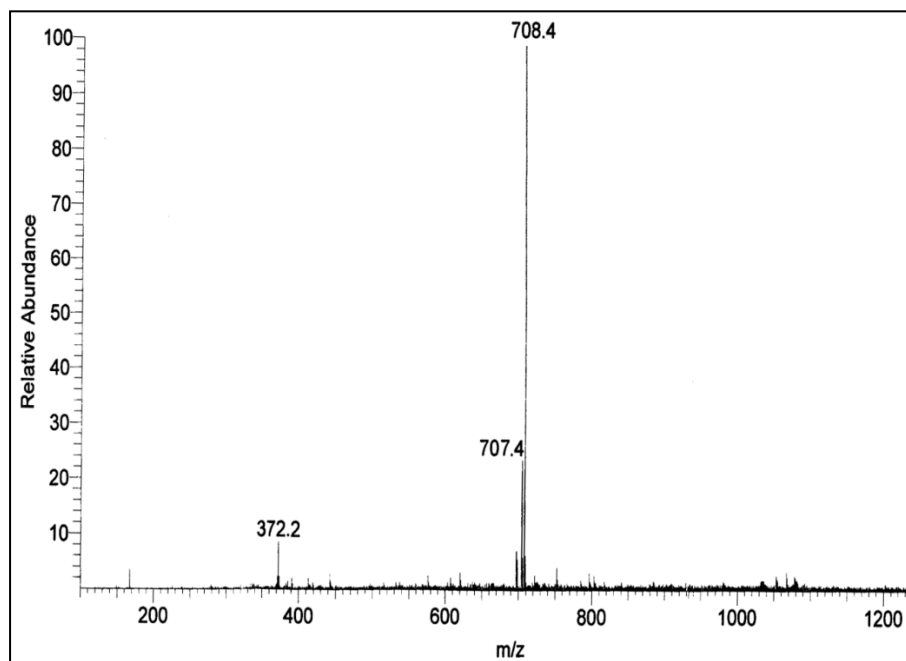


Figure S7a. ESI-MS spectrum of **5** in acetonitrile.

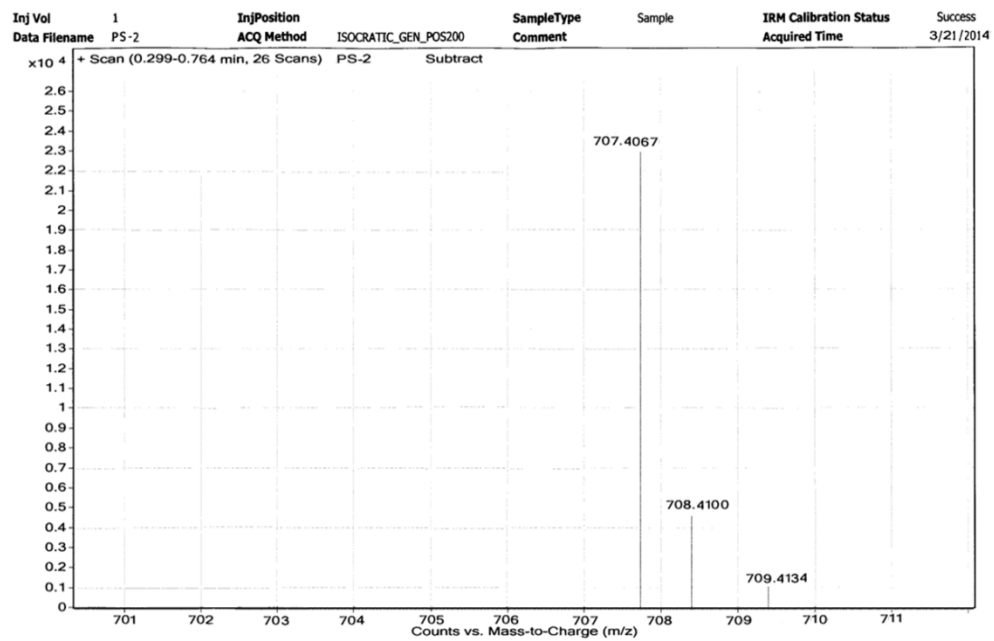


Figure S7b. HRMS spectrum of **5**.

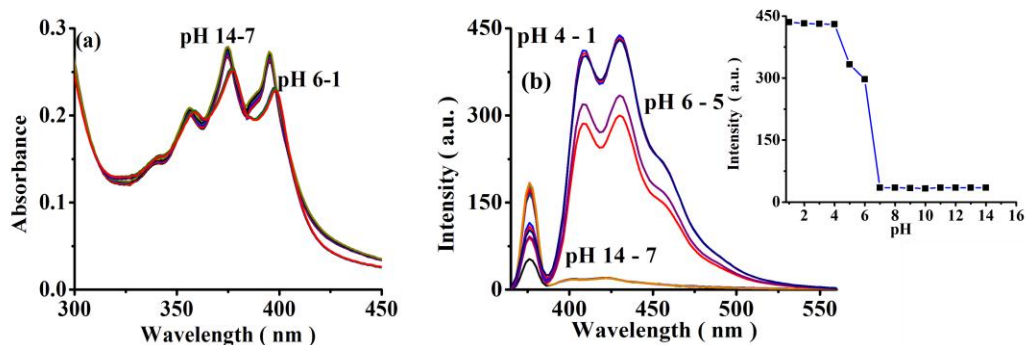


Figure S8. Relative change in (a) absorption and (b) emission spectra of **5** at different pH values 1-14, in HEPES buffer (10 mM; pH 7.0; 70% aqueous ACN). Inset: A pH-emission plot shows change in emission intensity of **5** at pH values, 1 to 14.

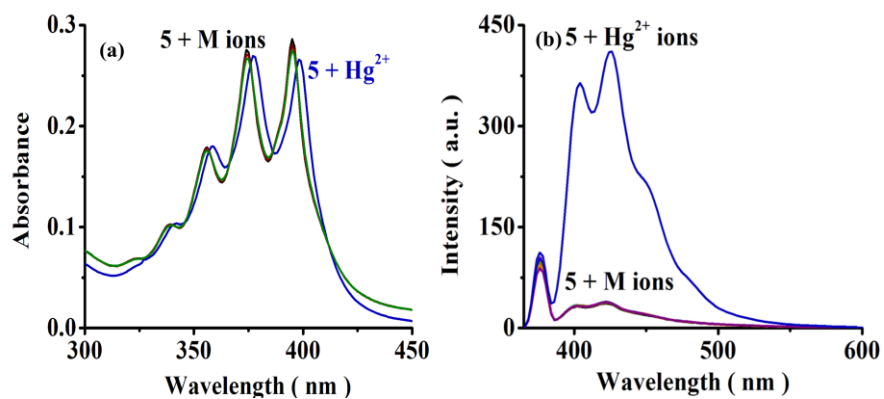


Figure S9: Change in (a) absorption (b) emission spectra of **5** (10 μ M) upon interaction with different metal ions (5.0 equiv) in HEPES buffer (10 mM; pH 7.0; 70% aqueous ACN).

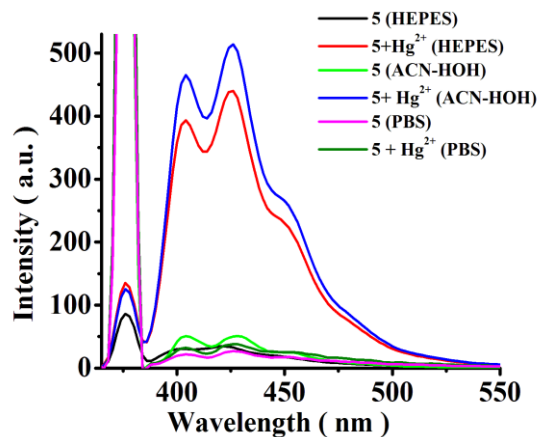


Figure S10. Emission spectra of **5** before and after addition of Hg^{2+} (2.5 equiv) in different medium; 70% aqueous-ACN, HEPES (10 mM; pH 7.0), and PBS (10 mM; pH 7.0) buffers.

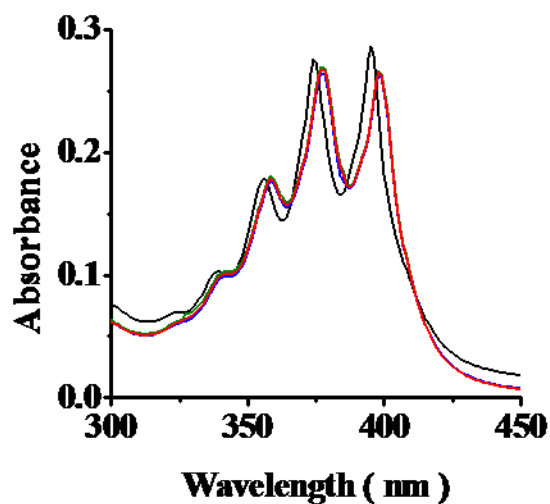


Figure S11. Change in the absorption spectra of a complex 5-Hg^{2+} , upon interference of tested cations in HEPES buffer (10 mM; pH 7.0; 70% aqueous ACN).

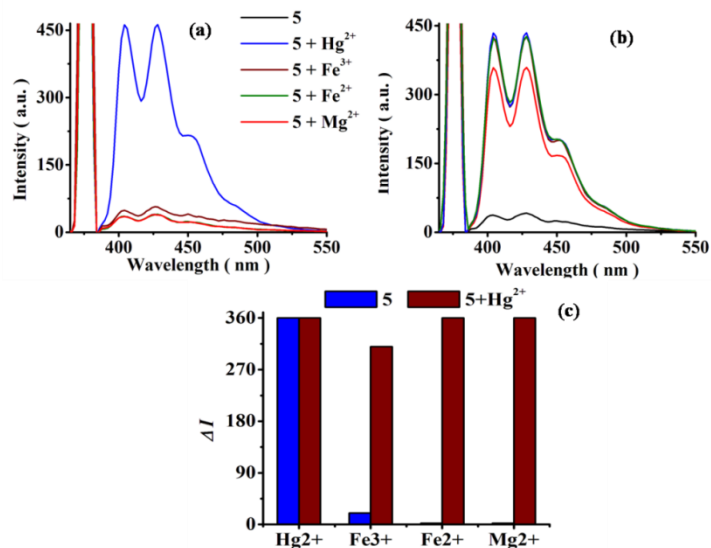


Figure S12. (a) Emission spectra of **5**, (b) Interference studies of 5+Hg^{2+} (2.5 equiv) upon interaction with Fe^{2+} , Fe^{3+} and Mg^{2+} ions (100 equiv) in HEPES buffer (10 mM; pH 7.0; 70% aqueous-ACN) and (c) Bar diagram shows change in emission intensity of **5** upon interaction and interference of tested cation.

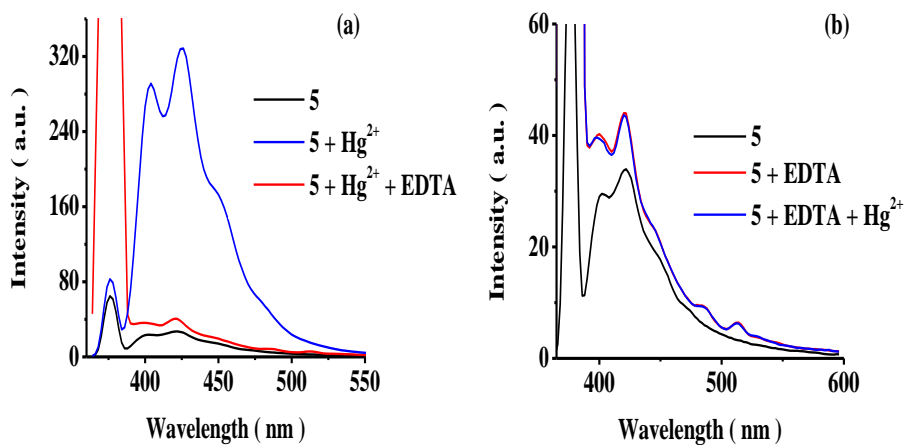


Figure S13. Change in the emission spectra of **5** by the addition of (a) EDTA to 5+Hg^{2+} ions (b) Hg^{2+} ions to 5+EDTA in HEPES buffer (10 mM; pH 7.0; 70% aqueous ACN).

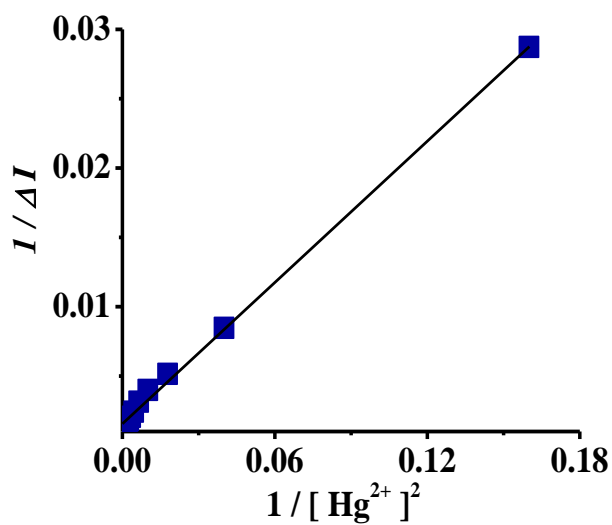


Figure S14. Benesi-Hildebrand plot for **5** and Hg^{2+} ions for a 1:2 binding stoichiometry in HEPES buffer (10 mM; pH 7.0; 70% aqueous ACN).

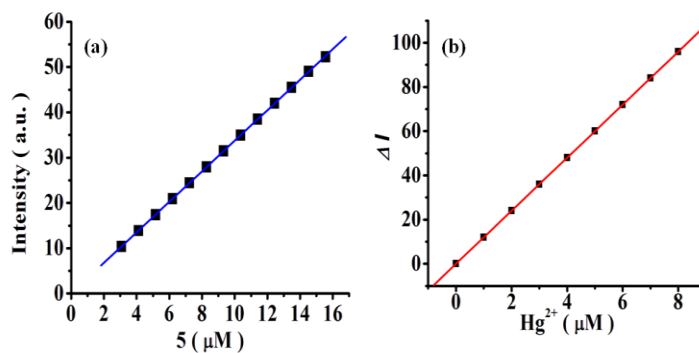


Figure S15. (a) Calibration curve for probe **5** and (b) calibration sensitivity plot of **5** toward Hg^{2+} ions in HEPES buffer (10 mM; pH 7.0; 70% aqueous-ACN).

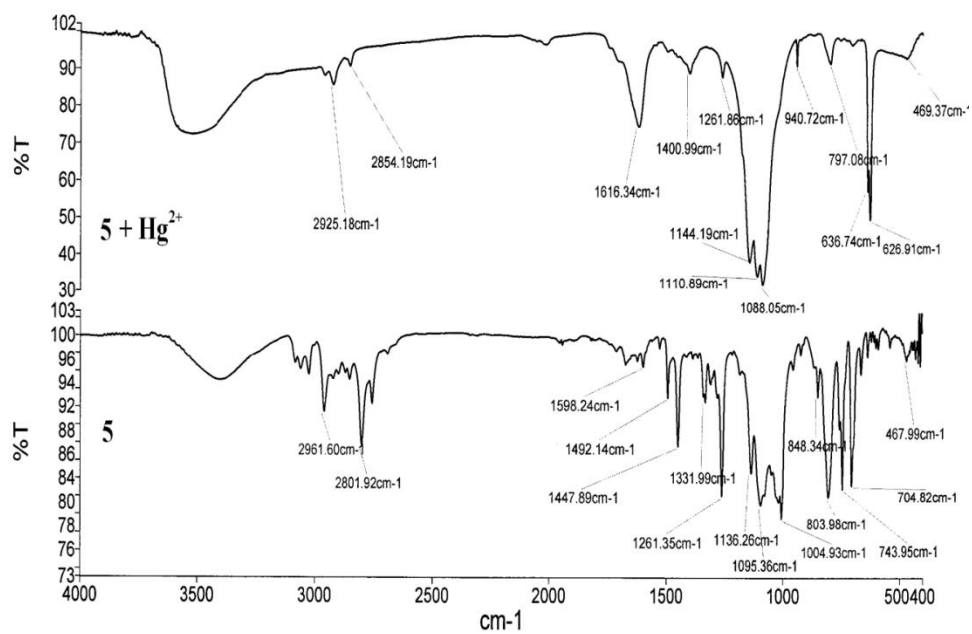


Figure S16. FT-IR spectrum of **5** and **5-Hg²⁺** complex.

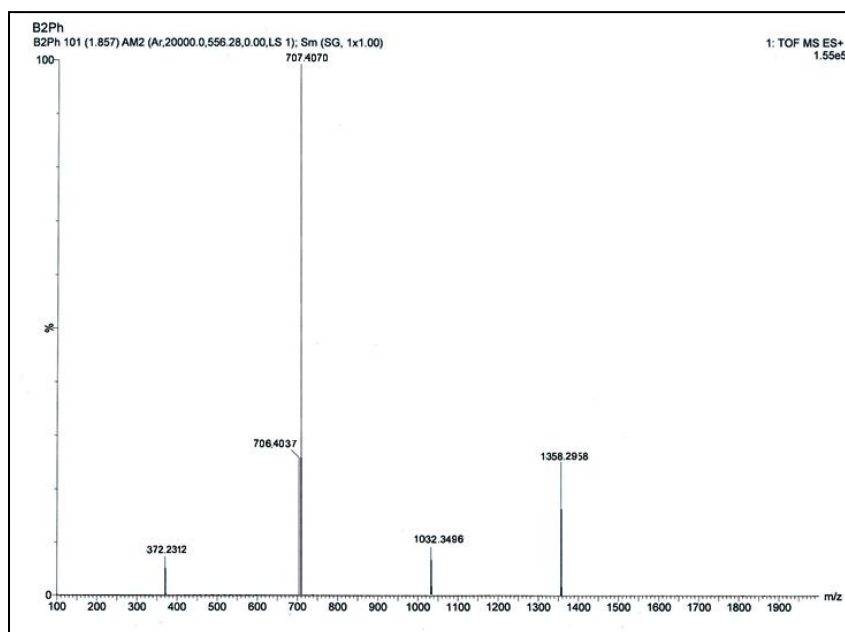


Figure S17. HRMS spectrum of **5-Hg²⁺** complex.

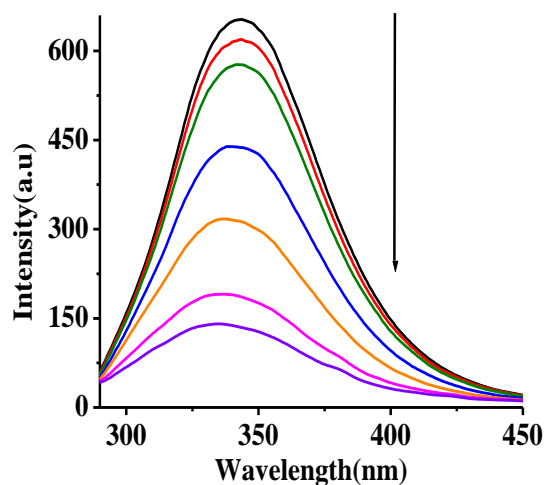


Figure S18. Emission titration experiment of BSA upon addition of Hg^{2+} ions (λ_{ex} 278 nm) in aqueous NaOAc buffer (50 mM; pH 6.7).

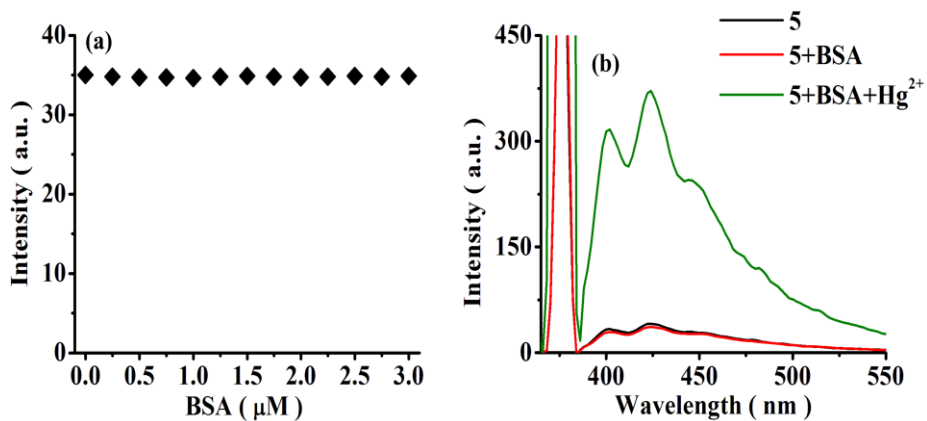


Figure S19. (a) Dependence of fluorescence intensity of probe **5** on BSA (0.0- 3.0 μM) and (b) Change in fluorescence spectra of **5** upon addition of BSA (2 μM) and Hg^{2+} (5.0 equiv) in HEPES buffer (10 mM; pH 7.0; 70% aqueous ACN).

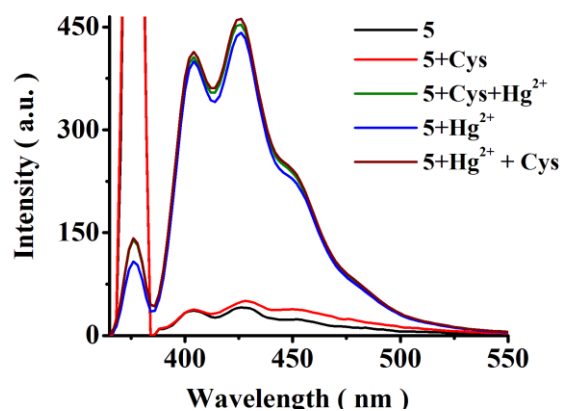


Figure S20. Emission spectra of **5** with Hg^{2+} acquired before and after addition of Cys in HEPES buffer (10 mM; pH 7.0; 70% aqueous ACN).

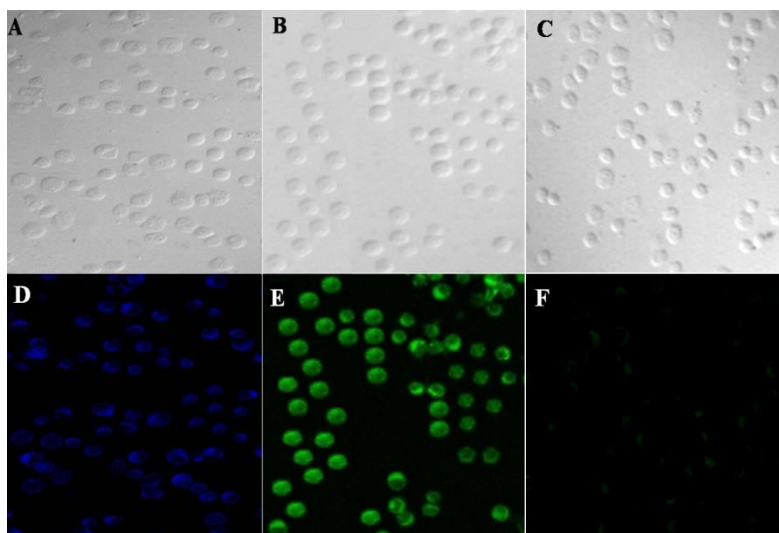


Figure S21. Confocal images of probe **5**+ M^{n+} ($\text{M}^{n+} = \text{Ca}^{2+}, \text{Fe}^{2+}, \text{Mg}^{2+}, \text{Zn}^{2+}$), **5**+ M^{n+} + Hg^{2+} and **5**+ M^{n+} + Hg^{2+} +TPEN (D, E and F; A, B and C are the DIC images of D, E and F respectively). Scale bar represents 100 μm .

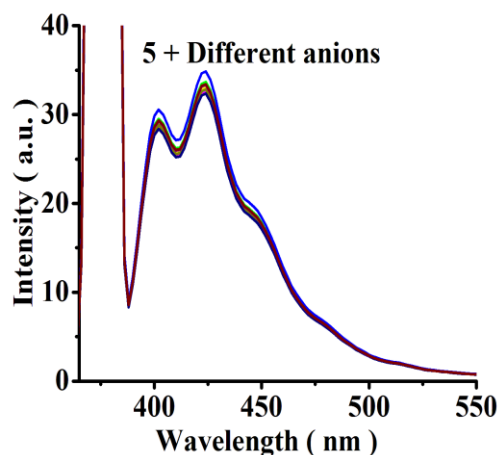


Figure S22. Change in emission spectra of **5** upon addition of different anions (50 equiv) in HEPES buffer (10 mM; pH 7.0; 70% aqueous ACN).

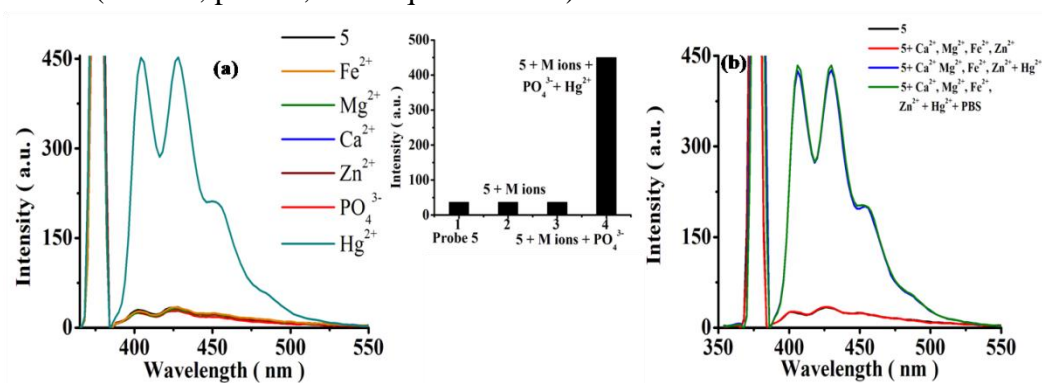


Figure S23. (a) Emission spectra of **5** (a) upon addition of M ions (Fe^{2+} , Mg^{2+} , Ca^{2+} , Zn^{2+} respectively) followed by PO_4^{3-} and finally Hg^{2+} . Inset : Bar diagram of interaction; (b) upon addition of M ions (Fe^{2+} , Mg^{2+} , Ca^{2+} , Zn^{2+} respectively) followed by Hg^{2+} and PBS in HEPES buffer (10 mM; pH 7.0; 70% aqueous ACN).

Logic interpretation: Considering applied chemical inputs of Hg^{2+} (5.0 equiv) and PO_4^{3-} (5.0 equiv) ions **5** exhibited low output emission in the absence (0 0) and presence (1 1) of both or only PO_4^{3-} (1 0) while in the presence of only Hg^{2+} (0 1) exhibit high output emission respectively. The truth table of resultant outputs construct an INHIBIT (output ‘A’) logic gate (Figure S24). Since, probe **5** in acidic medium ($\text{pH} \leq 6$) (In_3 , H^+) as well as in the presence of Hg^{2+} (In_2) exhibit enhanced, “turn-On” emission due to arrest in PET. Therefore, a combination of two inputs, of Hg^{2+} and H^+ as 1 0 or 0 1 or both 1 1 led to a high output emission (switched-On) while in the absence of both inputs (0 0) give low output fluorescence (switched-Off) and the truth table corresponds to an OR (output ‘B’) logic gate (Figure S25). Similarly, applying inputs of Hg^{2+} and EDTA as, 0 0, 1 1, or 0 1 always result low output emission while input 1 0 exhibited enhanced output emission, respectively and creates another INHIBIT (output ‘D’) logic gate (Figure S26). Notably probe **5** remains switched-on in acidic medium (In_3 , H^+), while switched-Off (low emission) by applying chemical inputs of either PO_4^{3-} or OH^- ions and a combination of different inputs (H^+ ; PO_4^{3-} or OH^-) in a truth table construct two INHIBIT (output ‘E’ and ‘F’) logic gates (Figure S27-28). Similarly, probe **5** is effective to detect Hg^{2+} in protein medium, BSA and helps to construct TRANSFER (output ‘C’) logic gate, as 0 0 or 0 1 exhibited low output emission while 1 1 or 1 0 give high output emission (Figure S29).

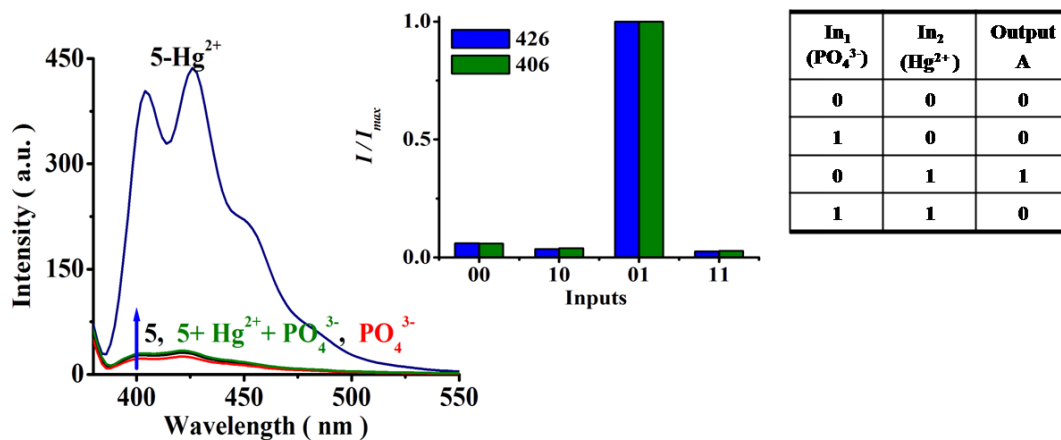


Figure S24. Emission spectra, bar diagram of relative intensities and truth table of INHIBIT logic gate of probe **5** upon applying inputs of PO₄³⁻ (In₁) and Hg²⁺ (In₂) ions in HEPES buffer (10 mM; pH 7.0; 70% aqueous ACN).

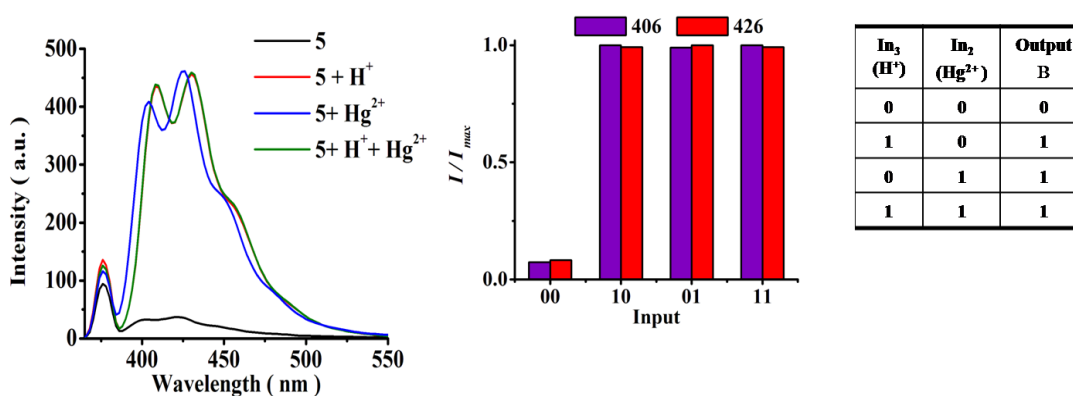


Figure S25. Emission spectra, bar diagram of relative intensities and truth table of OR logic gate of probe **5** upon applying inputs of Hg²⁺ (In₂) and H⁺ (In₃) ions in HEPES buffer (10 mM; pH 7.0; 70% aqueous ACN).

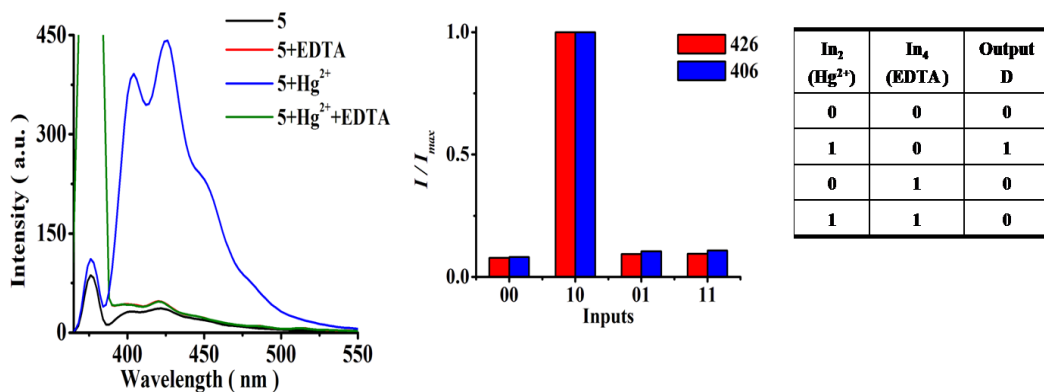


Figure S26. Emission spectra, bar diagram of relative intensities and truth table of INHIBIT logic gate of probe **5** upon applying inputs of Hg²⁺ (In₂) and EDTA (In₄) in HEPES buffer (10 mM; pH 7.0; 70% aqueous ACN).

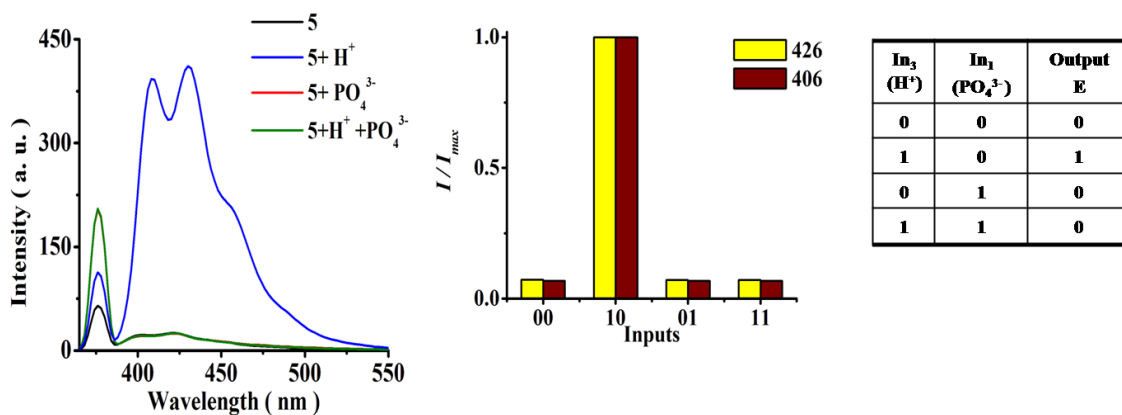


Figure S27. Emission spectra, bar diagram of relative intensities and truth table of INHIBIT logic gate of probe **5** upon applying inputs of H⁺ (In₃) and PO₄³⁻ (In₁) in HEPES buffer (10 mM; pH 7.0; 70% aqueous ACN).

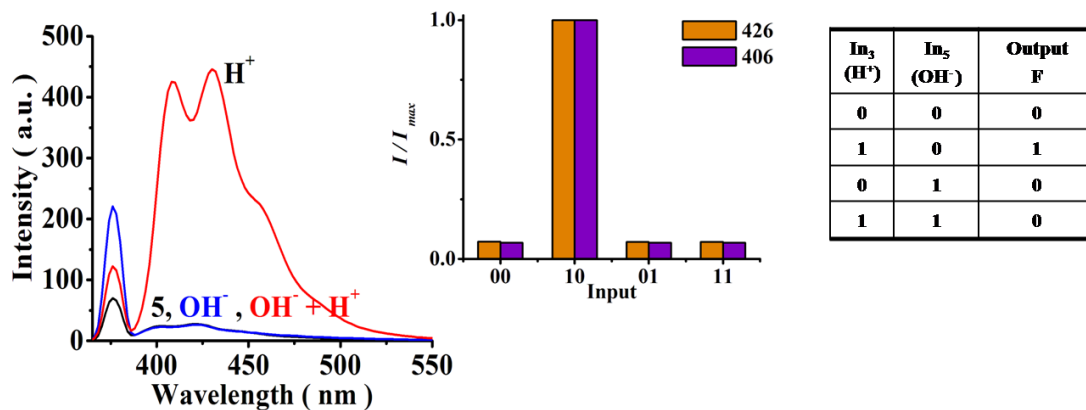


Figure S28. Emission spectra, bar diagram of relative intensities and truth table and symbol of INHIBIT logic gate of probe **5** upon applying inputs of H^+ (In_3) and OH^- (In_5) ions in HEPES buffer (10 mM; pH 7.0; 70% aqueous ACN).

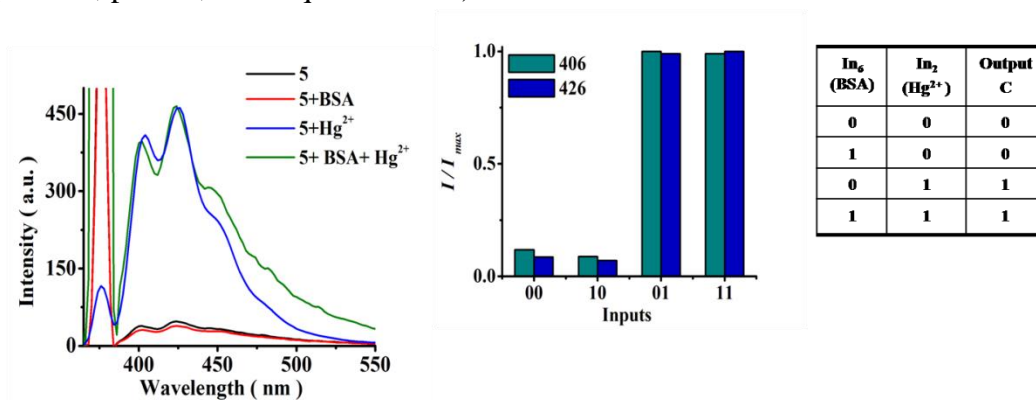


Figure S29. Emission spectra, bar diagram of relative intensities and truth table of TRANSFER logic gate of probe **5** upon applying inputs of BSA (In_6) and Hg^{2+} (In_2) in HEPES buffer (10 mM; pH 7.0; 70% aqueous ACN).

Table S1- Truth table of Three TRANSFER, one OR and one INHIBIT logic gate exhibited by probe 5.

In₇	In₈	output 'G'	In₉	In₁₀	output 'H'	In_C	In_H	output 'I'	In_I	In_{OH-}	output 'J'	In_J	In_{PO4³⁻}	output 'K'
0	0	0	0	0	0	0	0	0	0	0	0	0	0	0
1	0	0	1	0	1	1	0	1	1	0	1	1	0	1
0	1	1	0	1	0	0	1	1	0	1	0	0	1	0
1	1	1	1	1	1	1	1	1	1	1	1	1	1	0